NASA's Upcoming HyspIRI Mission –
Precision Vegetation Mapping with Limited Ground Truth

Saurabh Prasad [1], *Member, IEEE*, Lori M. Bruce [2], *Senior Member, IEEE*,

and Sathishkumar Samiappan

1. Assistant Research Professor, Mississippi State University, Mississippi State, MS 39762, saurabh.prasad@ieee.org
2. Professor, Mississippi State University, Mississippi State, MS 39762, bruce@ece.msstate.edu
3. Graduate Student, Mississippi State University

Availability of rich spectral information, as obtained from hyperspectral sensors, makes it possible to design ground cover classification systems that can perform highly accurate mapping and target recognition tasks [1], [2], [3]. Hyperspectral imaging is particularly powerful for vegetation species identification, growth stage monitoring, and stress characterization. HyspIRI, an NRC decadal survey mission, is much anticipated by researchers to aid in answering a wide variety of global ecological and anthropological questions. For example,

- What are the composition, function, and health of terrestrial and aquatic ecosystems?
- How are these ecosystems being altered by human activities and natural causes?
- How do these changes affect fundamental ecosystem processes upon which life on Earth depends? [4], [5]

In order to tackle these research topics and effectively exploit the seasonal global imaging spectroscopy provided by HyspIRI, there will be a great need for reliable hyperspectral-based products for use by domain experts. Arguably, easily accessible data products have been the key to the success of engaging domain experts and end-users in cases such as Landsat and MODIS. In those cases, simple multispectral products, such as NDVI, are well understood by both the mission teams and end-user communities. However, even though a great deal of research is conducted in hyperspectral image analysis, standard hyperspectral-based products do not currently exist.

In recent work [6], the authors generated "proxy" HyspIRI data from handheld Analytical Spectral Devices™ (ASD) [7] hyperspectral data. The handheld data was matched to the spectral specifications of the HyspIRI sensor. Figure 1 illustrates sample proxy HyspIRI signatures. The efficacy of current state-of-the-art land-cover classification systems (such as [8]) was studied on this proxy HyspIRI data. In this work, we will study the efficacy of HyspIRI observations in precision vegetation mapping applications, specifically aquatic invasive vegetation mapping, under limited ground-truth availability. In particular, sensitivity to the amount of training data, mixed pixel conditions, and temporal misalignments (training and testing on different phases of the phonological cycle of the vegetation) will be studied for a variety of conventional and state-of-the-art hyperspectral analysis techniques, such as principal component analysis (PCA), Fisher's linear discriminant analysis (LDA), stepwise linear discriminant analysis (SLDA) also known as discriminant analysis feature extraction (DAFE), and multi-classifier decision fusion (MCDF) systems. This study will provide valuable insight on the relationship between the quality and quantity of available ground-truth and performance of classification systems with these HyspIRI observations.

Furthermore, the authors will present results of the various hyperspectral analysis techniques' sensitivity to sensor error, for a variety of errors that could likely be present in HyspIRI data, such as symmetric failure (failure by frown), asymmetric failure by twist, and asymmetric failure by spectral-IFOV shift. Please see Figure 2. The authors intentionally introduce cross-track non-uniformity into the HyspIRI proxy data and quantify the sensitivity of the analysis techniques to these types of sensor error. This type of sensitivity analysis will be essential for utilizing existing hyperspectral analysis techniques during the actual HyspIRI mission. Figure 3 shows example results that will be included in this paper.

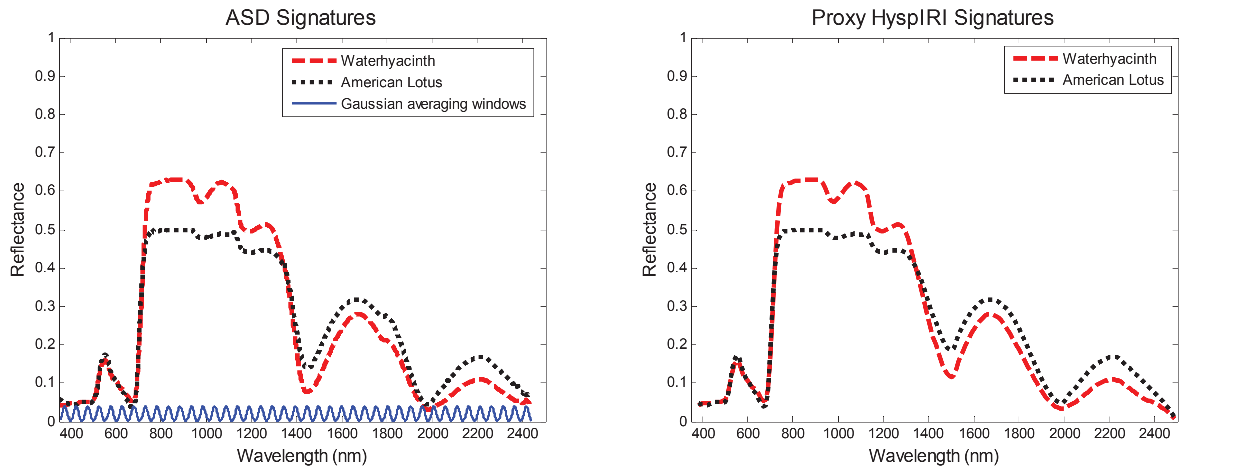

Figure 1: 2151 band ASD data and sample Gaussian averaging window locations (*left*), 212 band Proxy HyspIRI data generated from the ASD data (*right*) using the bank of averaging windows spaced 10nm apart, with a Full-Width Half Maximum (FWHM) bandwidth of 10nm.

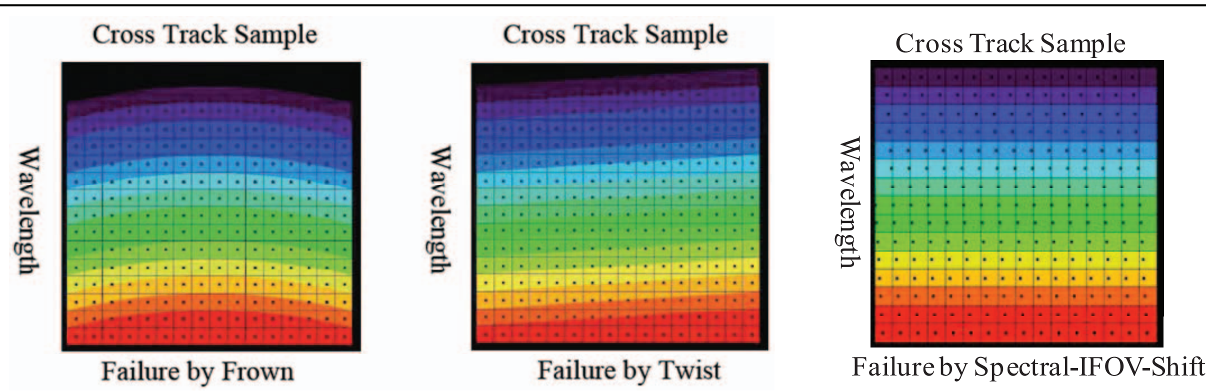

Figure 2. Illustration of two different modes of failure of cross-track uniformity. (Figure courtesy of Robert Green, 2007).

REFERENCES

[1] S. Kumar, J. Ghosh, M.M. Crawford, "Best-bases feature extraction algorithms for classification of hyperspectral data," in IEEE Transactions on Geoscience and Remote Sensing, Vol. 39, No. 7, pp 1368-1379, July 2001.

[2] S. Prasad, L.M. Bruce, "Hyperspectral feature space partitioning via mutual information for data fusion," in *Proceedings of IEEE Geoscience and Remote Sensing Symposium* , Barcelona, Spain, July 23-27, 2007.

[3] A. Cheriyadat, L.M. Bruce, A. Mathur, "Decision level fusion with best-bases for hyperspectral classification," in *Proceedings of IEEE Workshop on Advances in Techniques for Analysis of Remotely Sensed Data,* pp 399-406,October 2003.

[4] R. O. Green, "Overview of HyspIRI Mission" presented to the *International Spaceborne Imaging Spectroscopy Working Group*, 16 November 2007.

[5] R. O. Green, G. Asner, S. Ungar, R. Knox, "Results of the Decadal Survey HyspIRI Imaging Spectrometer concept study: A high signal-to-noise ratio and high

uniformity global mission to measure plant physiology and functional type," *in Proceedings of IEEE Geoscience and Remote Sensing Symposium*, Boston, MA, July 2008.

[6] S. Prasad, L. M. Bruce and H. Kalluri, "Data Exploitation of HyspIRI Observations for Precision Vegetation Mapping," in *IEEE Geoscience and Remote Sensing Symposium*, Cape Town, South Africa, 2009.

[7] Analytical Spectral Devices FieldspecPro FR specifications. Available: http://asdi.com/productsspecifications-FSP.asp.

[8] S. Prasad, L.M. Bruce, "Decision Fusion with Confidence based Weight Assignment for Hyperspectral Target Recognition," in *IEEE Transactions on Geoscience and Remote Sensing*, Vol. 46, No. 5, May 2008.

	% Overall Recognition Accuracy (95% Confidence Interval)			
Abundance	**PCA**	**LDA**	**SLDA**	**MCDF**
1	62.5 (1.6)	50.1 (1.7)	99.7 (0.2)	99.7 (0.2)
0.9	60.6 (1.6)	54.1 (1.7)	99.3 (0.2)	99.7 (0.2)
0.8	58.9 (1.6)	55.1 (1.7)	97.1 (0.5)	97.7 (0.5)
0.7	54.8 (1.7)	57.3 (1.6)	66.0 (1.5)	62.5 (1.6)
0.6	47.8 (1.7)	58.6 (1.6)	50.6 (1.6)	50.6 (1.6)
0.5	46.1 (1.7)	58.3 (1.6)	50.3 (1.7)	50.3 (1.7)
0.4	47.1 (1.7)	54.1 (1.7)	51.1 (1.7)	50.3 (1.7)
0.3	47.8 (1.7)	55.1 (1.7)	50.3 (1.7)	48.1 (1.7)
0.2	48.1 (1.7)	53.5 (1.7)	50.3 (1.7)	50.3 (1.7)
0.1	51.1 (1.7)	54.8 (1.7)	52.2 (1.7)	52.2 (1.7)
0	50.3 (1.7)	50.3 (1.7)	50.3 (1.7)	50.3 (1.7)

(a)

	% Overall Recognition Accuracy (95% Confidence Interval)			
Temporal Misalignment	**PCA**	**LDA**	**SLDA**	**MCDF**
±1 week	60.5 (1.6)	50.1 (1.7)	97.7 (0.4)	99.7 (0.2)
±2 week	58.6 (1.6)	54.1 (1.7)	97.1 (0.5)	97.7 (0.5)
±4 week	56.7 (1.7)	53.2 (1.7)	73.1 (1.0)	92.6 (0.5)
±6 week	52.8 (1.7)	52.3 (1.7)	72.2 (1.3)	74.5 (1.0)
±8 week	46.6 (1.7)	53.2 (1.7)	58.6 (1.6)	62.0 (1.5)

(b)

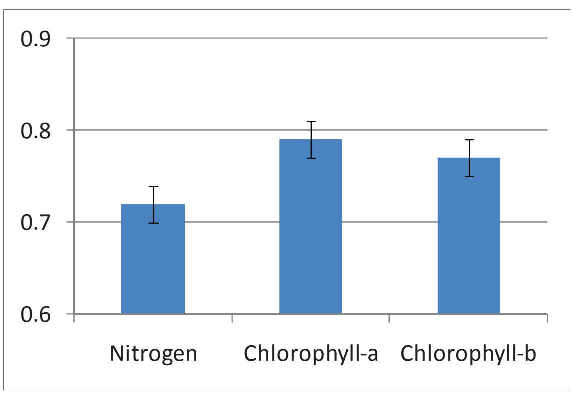

(c)

Figure 3: Example results of HyspIRI proxy data analysis. (a) Sensitivity of hyperspectral analysis technique to target abundance within pixel. (b) Sensitivity of hyperspectral analysis technique to temporal misalignment between ground truth data and satellite pass over. (c) R^2 values resulting from multivariate linear regression analysis of spectral band features with vegetation chemical content. Note: PCA – Principal Component Analysis, LDA – Fisher's Linear Discriminant Analysis, SLDA – Stepwise Linear Discriminant Analysis (also known as DAFE or Discriminant Analysis Feature Extraction), MCDF – Multi-Classifier Decision Fusion.